UNIVERSITY OF WEST BOHEMIA

Applied and Computational Mechanics 4 (2010) 37–48

Applied and Computational Mechanics

Modelling of the bladed disk vibration with damping elements in blade shroud

J. Kellner[a,*], V. Zeman[a]

[a] *Faculty of Applied Sciences, University of West Bohemia, Univerzitní 22, 306 14 Plzeň, Czech Republic*

Received 21 January 2010; received in revised form 19 July 2010

Abstract

The requirement for wide operation range of steam turbine can cause, that the blades work close to resonant frequency. For decreasing of blade's vibration there are placed damping elements in the blade shroud. These elements are calculated for dissipation of the vibration energy. The analytical method of blade and bladed disk modal analysis is introduced. The method enables to include blades both with and without damping elements in shroud. The mathematical model of the bladed disk is prepared for including damping effects in contact planes.

Keywords: bladed disk vibration, damping elements, modal properties

1. Introduction

The requirements on wide frequency operation range and mainly on higher efficiency of steam turbine blades lead to thinner profile, which is better in term of computation of fluid dynamics (CFD) but blade dynamic properties get worse. The purpose of damping elements is to decrease potential high amplitudes of blade vibration, which may occur due to resonances or big acting forces. The aim of this article is to develop suitable methodology for vibration modelling of damped blades. The method is based on discretization of 3D rotating disk [1] and 1D blades [3] by FEM. This contribution is the rudimentary step for research of dynamic behaviour of the bladed disk with damping elements, which are placed between blade shrouds using the harmonic (balance) linearization method. In future, the damping will be involve due to slip contact interaction in inner couplings between blade shrouds.

2. The mathematical modelling of the disk with blade foots

The rotating bladed disk (see fig. 1) can be generally decomposed into a disk (subsystem D) and separated blades (subsystems $B_i, i = 1, \ldots, r$). Disk is clamped on inner radius to rigid shaft rotating with constant angular velocity ω around its y axis. According to the derivation presented in [2] the disk can be discretized in the rotating $x\ y\ z$ coordinate system using linear isoparametric hexahedral finite elements (see [1]). The equation of motion can be written in a configuration space defined by the vector

$$\boldsymbol{q}_D = \left[\ldots, u_j^{(F)}, v_j^{(F)}, w_j^{(F)}, \ldots, u_j^{(C)}, v_j^{(C)}, w_j^{(C)}, \ldots\right]_D^T \in \mathcal{R}^{n_D} \tag{1}$$

*Corresponding author. Tel.: +420 732 556 838, e-mail: kennyk@kme.zcu.cz.

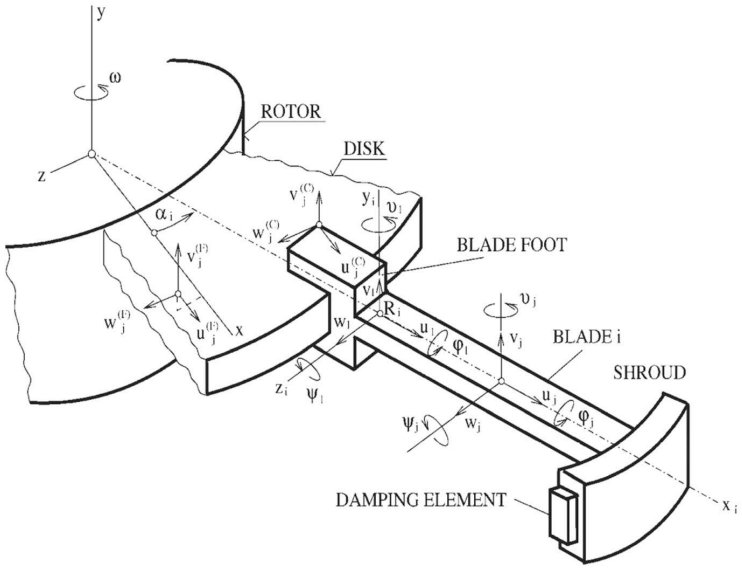

Fig. 1. Scheme of the rotating bladed disk

of nodal j displacements (see fig. 1) in direction of rotating axis x, y, z. The disk nodes are classified into free nodes (superscript F) and coupled nodes (superscript C) on the outer and inner surface of the blade foots. The mathematical model of the disk was derived in [1] using Lagrange's equations in the form

$$\boldsymbol{M}_D\ddot{\boldsymbol{q}}_D(t) + \omega\boldsymbol{G}_D\dot{\boldsymbol{q}}_D(t) + \left(\boldsymbol{K}_{sD} - \omega^2\boldsymbol{K}_{dD}\right)\boldsymbol{q}_D(t) = \omega^2\boldsymbol{f}_D\,, \tag{2}$$

where $\boldsymbol{M}_D$, $\boldsymbol{K}_{sD}$ and $\boldsymbol{K}_{dD}$ are symmetric mass, static stiffness and dynamic softening matrices, skew-symmetric matrix $\omega\boldsymbol{G}_D$ expresses gyroscopic effects and $\omega^2\boldsymbol{f}_D$ is force vector of centrifugal load.

The vector of generalized coordinates of the disk can be partitioned according to (1) as

$$\boldsymbol{q}_D = \begin{bmatrix} \boldsymbol{q}_D^{(F)} \\ \boldsymbol{q}_D^{(C)} \end{bmatrix},\ \boldsymbol{q}_D^{(F)} \in \mathcal{R}^{n_D^{(F)}},\ \boldsymbol{q}_D^{(C)} \in \mathcal{R}^{n_D^{(C)}}\,. \tag{3}$$

The displacements of the coupled disk nodes on condition of rigid blade foots modelled as a disk part can be expressed by displacements of referential nodes R_i which are identical with the first blade nodes $j = 1$ at blade foots (see fig. 1). This relation between coupled disk displacements corresponding to blade i and blade displacements in referential node R_i is

$$\begin{bmatrix} u_j^{(C)} \\ v_j^{(C)} \\ w_j^{(C)} \end{bmatrix} = \begin{bmatrix} \cos\alpha_i & 0 & \sin\alpha_i \\ 0 & 1 & 0 \\ -\sin\alpha_i & 0 & \cos\alpha_i \end{bmatrix} \left[\begin{array}{ccc|ccc} 1 & 0 & 0 & 0 & z_j & -y_j \\ 0 & 1 & 0 & -z_j & 0 & x_j \\ 0 & 0 & 1 & y_j & -x_j & 0 \end{array}\right] \begin{bmatrix} u_1 \\ v_1 \\ w_1 \\ \varphi_1 \\ \vartheta_1 \\ \psi_1 \end{bmatrix}_{B,i}, \tag{4}$$

or shortly

$$\boldsymbol{q}_j^{(C)} = \boldsymbol{T}_{\alpha_i}\boldsymbol{T}_j\boldsymbol{q}_{1,i}, \qquad i = 1, 2, \ldots, r, \tag{5}$$

where $x_j,\ y_j,\ z_j$ are coordinates of the coupled disk node j on the rigid blade foots in coordinate system x_i, y_i, z_i of the blade i with the origin in the first blade node and α_i is the angle between the rotating disk axis x and the rotating blade axis x_i. Coordinates of vector $\boldsymbol{q}_{1,i}$ express the referential node displacements in direction of blade rotating axes x_i, y_i, z_i and small turn angles of the blade cross section in node R_i.

The complete transformation between displacements of coupled nodes of the disk on the blade foots and the referential nodes R_i of all blades can be expressed in the matrix form

$$\left[\begin{array}{c} \vdots \\ \hline \boldsymbol{q}_j^{(C)} \\ \hline \vdots \end{array}\right] = \left[\begin{array}{c|c|c} & \vdots & \\ \hline \ldots & \boldsymbol{T}_{\alpha_i}\boldsymbol{T}_j & \ldots \\ \hline & \vdots & \end{array}\right] \left[\begin{array}{c} \vdots \\ \hline \boldsymbol{q}_{1,i} \\ \hline \vdots \end{array}\right] \Rightarrow \boldsymbol{q}_D^{(C)} = \boldsymbol{T}_{D,R}\boldsymbol{q}_R\,. \tag{6}$$

The global transformation rectangular matrix $\boldsymbol{T}_{D,R} \in \mathcal{R}^{n_D^{(C)},n_R}$ describes the linkage between the disk (D) and the blade rim (R). Coordinates of vector $\boldsymbol{q}_R$ express displacements of the blade nodes $j = 1, 2, \ldots, N$ (see below) in coordinate systems x_i, y_i, z_i (see fig. 1) in order of blades (for $i = 1, 2, \ldots, r$)

$$\boldsymbol{q}_R = \left[\boldsymbol{q}_{B,1}^T \quad \boldsymbol{q}_{B,2}^T \quad \ldots \boldsymbol{q}_{B,r}^T\right]^T \in \mathcal{R}^{n_R}, \qquad n_R = 6Nr, \tag{7}$$

where r is the blade number.

For illustration we present in table 2a number of lowest natural frequencies of the nonrotating centrally clamped modeled disk (see fig. 2) with rigid blade foots but without blades. The nodes which lie on the inner radius are fixed in all directions. The mode shapes corresponding to natural frequencies are characterized by the number of nodal diameters (ND) and the number of nodal circles (NC). the modal values of the disk with foots modelled as flexible differ from the disk model with rigid foots very small [4].

Table 1. Parameters of model

Disk width	9 mm
Disk outer radius	252.5 mm
Number of blades	60 pcs
Length of blade	205 mm
Width of blade	20 mm
Hight of blade	10 mm
Shroud mass	0.078 kg

Table 2. Modal analysis of the disk with rigid blade foots

Frequencies of disk with blade foots		
	[Hz]	shape
1	234,8	1 ND
2	234,8	1 ND
3	249,8	1 NC
4	306,7	2 ND
5	306,7	2 ND
6	599,3	3 ND
7	599,3	3 ND

3. The blade rim with damping elements in shroud

The single blades are modelled as one dimensional continuum linked with rigid shroud body in its centre of gravity of last blade profile. The mathematical model of the uncoupled blade i with shroud in configuration space of its blade node displacements (in the direction of rotating axes x_i, y_i, z_i and of small angular displacements of the blade cross sections)

$$\boldsymbol{q}_{B,i} = [\ldots, u_j, v_j, w_j, \varphi_j, \vartheta_j, \psi_j, \ldots]_{B,i}^T \in \mathcal{R}^{n_B},\ i = 1, 2, \ldots, r; j = 1, 2, \ldots, N \tag{8}$$

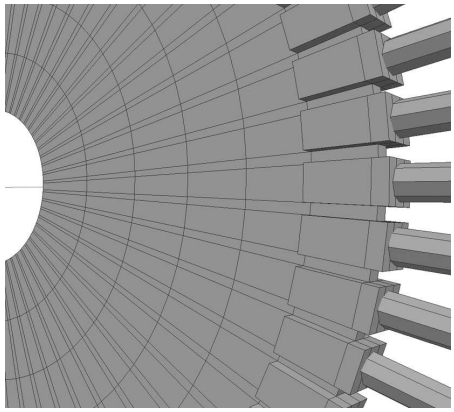

Fig. 2. Scheme of the disk with blade foots

has the form [3, 5]

$$\boldsymbol{M}_B\ddot{\boldsymbol{q}}_{B,i}(t) + \omega\boldsymbol{G}_B\dot{\boldsymbol{q}}_{B,i}(t) + \left(\boldsymbol{K}_{sB} + \omega^2\boldsymbol{K}_{\omega B} - \omega^2\boldsymbol{K}_{dB}\right)\boldsymbol{q}_{B,i}(t) = \omega^2\boldsymbol{f}_B\,, \tag{9}$$

where blade matrices $\boldsymbol{M}_B$, $\boldsymbol{K}_{sB}$, $\boldsymbol{K}_{dB}$ and $\boldsymbol{G}_B$ have an identical meaning with matrices of the disk and matrix $\omega^2\boldsymbol{K}_{\omega,B}$ expresses a centrifugal blade stiffening. (Shortly, the deformation energy gained due to extension in centrifugal array can be expressed by matrix of blade centrifugal stiffening [5]-Appendix 1.) The matrix $\boldsymbol{K}_{dB}$ is result of modelling of 1D continuum in rotating coordinate system.

In this first modelling task is supposed, that the damping element is fast connected on the sloping side with blade $i+1$ because the frictional force here is much higher than on the straight (radial) side of the damping element. This model in the first step of modelling respects only a contact stiffness between blade i and damping element connected with following blade $i+1$ on the radial area. This contact stiffness is defined by contact stiffness matrix between blades i and $i+1$

$$\mathbf{K}_C^{(B)} = \mathrm{diag}\,(0 \quad 0 \quad k_\zeta \quad k_{\xi\xi} \quad k_{\eta\eta} \quad 0)_{\xi_i,\eta_i,\zeta_i}\,, \tag{10}$$

expressing the constraint for the circumferential displacement and two rotations by means of contact stiffness k_ζ in normal direction to radial area $\xi_i\eta_i$ and two flexural stiffnesses $k_{\xi\xi},\ k_{\eta\eta}$.

This contact stiffness matrix is expressed in local contact coordinate system ξ_i, η_i, ζ_i placed in central contact point B_i of the i-th blade shroud. The coupling (deformation) energy between two adjacent blades i and $i+1$ (see fig. 3 is, in this contact coordinate system, expressed as

$$E_C^{i,i+1} = \frac{1}{2}\left(\boldsymbol{q}_{B_i} - \boldsymbol{q}_{A_{i+1}}\right)^T_{\xi_i,\eta_i,\zeta_i}\mathbf{K}_C^{(B)}\left(\boldsymbol{q}_{B_i} - \boldsymbol{q}_{A_{i+1}}\right)_{\xi_i,\eta_i,\zeta_i}\,, \tag{11}$$

where $\boldsymbol{q}_{B_i}, \boldsymbol{q}_{A_{i+1}}$ are vectors of blade i displacements in point B_i and blade $i+1$ displacements in pointA_{i+1} expressed in coordinate system ξ_i, η_i, ζ_i. The difference between $\boldsymbol{q}_{B_i} - \boldsymbol{q}_{A_{i+1}}$ represents the relative motion of contact areas between two adjacent blades i and $i+1$.

The translation of blade local coordinate systems from point C_i to point B_i and from point C_{i+1} to point A_{i+1} is expressed by translation matrices

$$\boldsymbol{R}_X^T = \begin{bmatrix} 0 & z_X & -y_X \\ -z_X & 0 & x_X \\ y_X & -x_X & 0 \end{bmatrix}, \quad X = A_{i+1}, B_i. \tag{12}$$

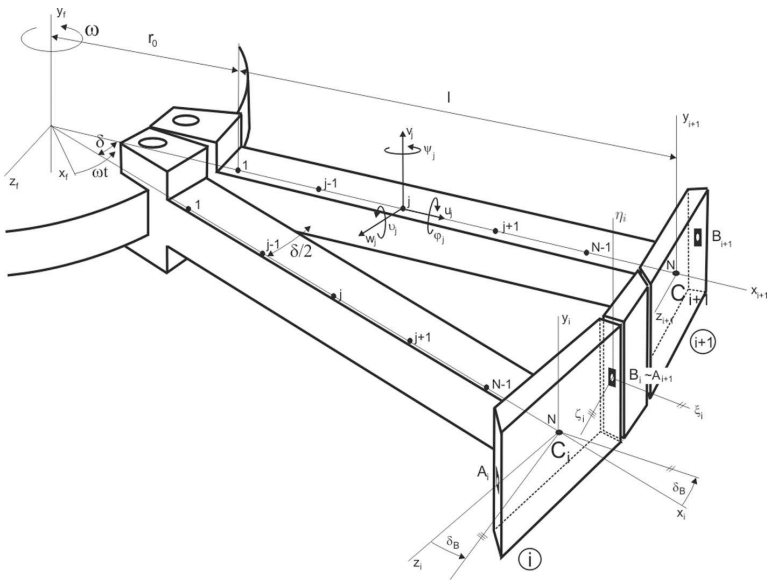

Fig. 3. Scheme of two adjacent blades and damping element

The translated local coordinate system is then rotated so, that the contact coordinate axis ξ_i is the radial according to bladed disk axis of rotation y_f.

The vector of displacements in point B_i in the contact coordinate system is

$$\boldsymbol{q}_{B_i\ \xi_i,\eta_i,\zeta_i} = \begin{bmatrix} u_{B_i} \\ v_{B_i} \\ w_{B_i} \\ \varphi_{B_i} \\ \vartheta_{B_i} \\ \psi_{B_i} \end{bmatrix}_{\xi_i,\eta_i,\zeta_i} = \left[\begin{array}{c|c} \boldsymbol{\tau}_B & \mathbf{0} \\ \hline \mathbf{0} & \boldsymbol{\tau}_B \end{array}\right] \begin{bmatrix} u_{B_i} \\ v_{B_i} \\ w_{B_i} \\ \varphi_{B_i} \\ \vartheta_{B_i} \\ \psi_{B_i} \end{bmatrix}_{x_i,z_i,y_i} \begin{matrix} \Big\} \mathbf{u}_{B_i} \\ \Big\} \boldsymbol{\varphi}_{B_i} \end{matrix} \Big\} \boldsymbol{q}_{B_i\ x_i,y_i,z_i}, \tag{13}$$

where the rotation matrix $\boldsymbol{\tau}_B$ between coordinate systems is specified by angle δ_B between radial axis x_i of blade passing through point C_i and radial axis ξ_i passing through point B_i.

$$\boldsymbol{\tau}_B = \begin{bmatrix} \cos\delta_B & 0 & -\sin\delta_B \\ 0 & 1 & 0 \\ \sin\delta_B & 0 & \cos\delta_B \end{bmatrix}. \tag{14}$$

Analogously the vector of displacements of point A_{i+1} in this contact coordinate system is defined as

$$\boldsymbol{q}_{A_{i+1}\ \xi_i,\eta_i,\zeta_i} = \begin{bmatrix} \boldsymbol{\tau}_A & \mathbf{0} \\ \mathbf{0} & \boldsymbol{\tau}_A \end{bmatrix} \boldsymbol{q}_{A_{i+1}\ x_{i+1},y_{i+1},z_{i+1}}, \tag{15}$$

where

$$\boldsymbol{\tau}_A = \begin{bmatrix} \cos\delta_A & 0 & \sin\delta_A \\ 0 & 1 & 0 \\ -\sin\delta_A & 0 & \cos\delta_A \end{bmatrix}. \tag{16}$$

The vector of blade i displacements in point B_i in coordinate system x_i, y_i, z_i is defined by generalized displacements of point C_i and by matrix of translation $\boldsymbol{R}_B$

$$\boldsymbol{q}_{B_i\ x_i,y_i,z_i} = \left[\begin{array}{c} \boldsymbol{u}_{B_i} \\ \boldsymbol{\varphi}_{B_i} \end{array}\right]_{x_i,y_i,z_i} = \left[\begin{array}{cc} \boldsymbol{E} & \boldsymbol{R}_B^T \\ \boldsymbol{0} & \boldsymbol{E} \end{array}\right] \left[\begin{array}{c} \boldsymbol{u}_{C_i} \\ \boldsymbol{\varphi}_{C_i} \end{array}\right]_{x_i,y_i,z_i} = \left[\begin{array}{cc} \boldsymbol{E} & \boldsymbol{R}_B^T \\ \boldsymbol{0} & \boldsymbol{E} \end{array}\right] \boldsymbol{q}_{C_i}. \tag{17}$$

According to (13) this vector in the contact coordinate system ξ_i, η_i, ζ_i has the form

$$\boldsymbol{q}_{B_i\ \xi_i,\eta_i,\zeta_i} = \underbrace{\left[\begin{array}{cc} \boldsymbol{\tau_B} & \boldsymbol{0} \\ \boldsymbol{0} & \boldsymbol{\tau}_B \end{array}\right] \left[\begin{array}{cc} \boldsymbol{E} & \boldsymbol{R}_B^T \\ \boldsymbol{0} & \boldsymbol{E} \end{array}\right]}_{\boldsymbol{T}_B} \boldsymbol{q}_{C_i\ x_i,y_i,z_i}. \tag{18}$$

Analogously, the vector of blade $i+1$ displacements in point A_{i+1} in the contact coordinate system ξ_i, η_i, ζ_i is expressed as

$$\boldsymbol{q}_{A_{i+1}\ \xi_i,\eta_i,\zeta_i} = \underbrace{\left[\begin{array}{cc} \boldsymbol{\tau_A} & \boldsymbol{0} \\ \boldsymbol{0} & \boldsymbol{\tau}_A \end{array}\right] \left[\begin{array}{cc} \boldsymbol{E} & \boldsymbol{R}_A^T \\ \boldsymbol{0} & \boldsymbol{E} \end{array}\right]}_{\boldsymbol{T}_A} \boldsymbol{q}_{C_{i+1}\ x_{i+1},y_{i+1},z_{i+1}}. \tag{19}$$

We can now express the coupling energy, defined in (11)by means of generalized coordinates of i-th and $i+1$-th blades in the form

$$E_C^{i,i+1} = \frac{1}{2} \left(\boldsymbol{T}_B \boldsymbol{q}_{C_i} - \boldsymbol{T}_A \boldsymbol{q}_{C_{i+1}}\right)^T \mathbf{K}_C^{(B)} \left(\boldsymbol{T}_B \boldsymbol{q}_{C_i} - \boldsymbol{T}_A \boldsymbol{q}_{C_{i+1}}\right). \tag{20}$$

After multiplying the previous equation and from identity $\frac{\partial E_C^{i,i+1}}{\partial \boldsymbol{q}_R} = \boldsymbol{K}_{C_i}^{(R)} \boldsymbol{q}_R$ we obtain the stiffness matrix of coupling between two adjacent blades i and $i+1$ in the form

$$\mathbf{K}_{C_i}^{(R)} = \begin{array}{c} \\ \\ \\ \\ \\ \\ \\ \end{array} \begin{array}{c} \begin{array}{ccccc} & \boldsymbol{q}_{C_i}^T & & \boldsymbol{q}_{C_{i+1}}^T & \end{array} \\ \left[\begin{array}{c|c|c|c|c} \vdots & & \vdots & & \vdots \\ \hline \cdots & \overbrace{\mathbf{T}_B^T \mathbf{K}_C^{(B)} \mathbf{T}_B}^{\mathbf{K}_{B,B}} & \cdots & \overbrace{-\mathbf{T}_B^T \mathbf{K}_C^{(B)} \mathbf{T}_A}^{-\mathbf{K}_{B,A}} & \cdots \\ \hline \vdots & & \vdots & & \vdots \\ \hline \cdots & \overbrace{-\mathbf{T}_A^T \mathbf{K}_C^{(B)} \mathbf{T}_B}^{-\mathbf{K}_{A,B}} & \cdots & \overbrace{\mathbf{T}_A^T \mathbf{K}_C^{(B)} \mathbf{T}_A}^{\mathbf{K}_{A,A}} & \cdots \\ \hline \vdots & & \vdots & & \vdots \end{array}\right] \end{array} \begin{array}{l} \\ \\ \\ \\ \\ \\ \\ \end{array} \begin{array}{l} \\ \boldsymbol{q}_{C_i} \\ \\ \\ \\ \boldsymbol{q}_{C_{i+1}} \\ \\ \end{array} \begin{array}{l} \\ \\ \left.\begin{array}{l} \\ \\ \end{array}\right\} \boldsymbol{q}_{B,i} \\ \\ \left.\begin{array}{l} \\ \\ \end{array}\right\} \boldsymbol{q}_{B,i+1} \\ \\ \end{array}, \tag{21}$$

where $\boldsymbol{q}_{B,i}$ and $\boldsymbol{q}_{B,i+1}$ are the vectors of all generalized displacements of blade i and i-th. Vectors $\boldsymbol{q}_{C_i}$ and $\boldsymbol{q}_{C,i+1}$ are the vectors of generalized displacements in the last node N on blade i and i-th, respectively.

The whole coupling stiffness matrix between all blades (here 60 blades) is then

$$\mathbf{K}_C^{(R)} = \begin{array}{c} \begin{array}{ccccccccccc} & \boldsymbol{q}_{C_1}^T & & \boldsymbol{q}_{C_2}^T & & \boldsymbol{q}_{C_3}^T & & & \boldsymbol{q}_{C_{59}}^T & & \boldsymbol{q}_{C_{60}}^T \end{array} \\ \left[\begin{array}{ccccccccccc} \vdots & & \vdots & & \vdots & & \vdots & & \vdots & \\ \cdots & \mathbf{K}_{A,A}+\mathbf{K}_{B,B} & \cdots & -\mathbf{K}_{B,A} & \cdots & & \cdots & & \cdots & -\mathbf{K}_{A,B} \\ \vdots & & \vdots & & \vdots & & \vdots & & \vdots & \\ \cdots & -\mathbf{K}_{A,B} & \cdots & \mathbf{K}_{A,A}+\mathbf{K}_{B,B} & \cdots & -\mathbf{K}_{B,A} & \cdots & & \cdots & \\ \vdots & & \vdots & & \vdots & & \vdots & & \vdots & \\ \cdots & & \cdots & -\mathbf{K}_{A,B} & \cdots & \mathbf{K}_{A,A}+\mathbf{K}_{B,B} & \cdots & -\mathbf{K}_{B,A} & & \\ \approx & \approx & \approx & \approx & \approx & \approx & \approx & \approx & \approx & \approx \\ \vdots & & \vdots & & \vdots & & \vdots & & \vdots & \\ \cdots & & \cdots & & \cdots & & \cdots & \mathbf{K}_{A,A}+\mathbf{K}_{B,B} & \cdots & -\mathbf{K}_{B,A} \\ \vdots & & \vdots & & \vdots & & \vdots & & \vdots & \\ \cdots & -\mathbf{K}_{B,A} & \cdots & & \cdots & & \cdots & -\mathbf{K}_{A,B} & & \mathbf{K}_{A,A}+\mathbf{K}_{B,B} \end{array}\right] \end{array} . \tag{22}$$

This contact stiffness matrix connects the blades together into a blade rim, whose equation of motion is

$$\boldsymbol{M}_R\ddot{\boldsymbol{q}}_R(t) + \omega\boldsymbol{G}_R\dot{\boldsymbol{q}}_R(t) + \left(\boldsymbol{K}_{sR} + \boldsymbol{K}_C^{(R)} + \omega^2\boldsymbol{K}_{\omega R} - \omega^2\boldsymbol{K}_{dR}\right)\boldsymbol{q}_R(t) = \omega^2\boldsymbol{f}_R\,, \tag{23}$$

where all matrices (except $\boldsymbol{K}_C^{(R)}$ are block-diagonal in the form

$$\boldsymbol{X}_R = \mathrm{diag}\left(\boldsymbol{X}_B,\, \boldsymbol{X}_B,\, \ldots,\, \boldsymbol{X}_B\right), \quad \boldsymbol{X} = \boldsymbol{M}, \boldsymbol{G}, \boldsymbol{K}_s, \boldsymbol{M}_d, \boldsymbol{K}_\omega. \tag{24}$$

The contact stiffness matrix $\boldsymbol{K}_C^{(B)}$ defined in (10) depends on geometric and material characteristics of damping element. Mentioned above, the frictional force is much higher on the slopping side, so at the first time the damping element is considered fast connect here. The normal force in the contact on radial straight side is

$$N_0 = \frac{m_T r\omega^2}{\tan\delta_\alpha}, \tag{25}$$

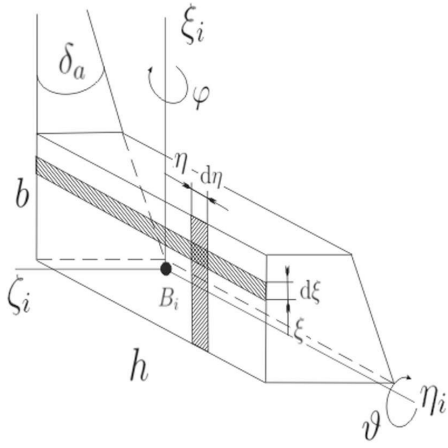

Fig. 4. Scheme of the damping element

where m_T is the damping element mass, $\omega = \frac{\pi n}{30}$ is the angular velocity and r is radius of damping element centre of gravity. The contact stress is

$$\sigma_{[MPa]} = \frac{N_{0\,[N]}}{A_{ef\,[mm^2]}}, \quad A_{ef} = \overbrace{h\gamma_h}^{h_{ef}} \overbrace{b\gamma_b}^{b_{ef}} \cdot 10^6, \tag{26}$$

where h is axial and b is radial damping element proportions and A_{ef} is the effective contact area (see fig. 4), defined by real size of contact area, i.e. the high h multiply by coefficient γ_h etc.

The contact normal stiffness in direction ζ is

$$k_\zeta = \frac{N_0}{\delta} \cdot 10^6 [N/m], \tag{27}$$

where contact deformation $\delta_{[\mu m]} = c\sigma^p$ in μm is defined, according to [6], by contact deformation coefficient c and contact exponent p. Moments of flexion around axes ξ_i and η_i can be expressed as

$$\begin{aligned} M_\xi &= 2\int_0^{h_{ef}/2} k_I b_{ef} \mathrm{d}\eta\, \eta^2 \varphi = \frac{1}{12} \underbrace{k_I b_{ef} h_{ef}}_{k_\zeta} h_{ef}^2 \varphi, \\ M_\eta &= 2\int_0^{b_{ef}/2} k_I h_{ef} \mathrm{d}\xi\, \xi^2 \varphi = \frac{1}{12} \underbrace{k_I b_{ef} h_{ef}}_{k_\zeta} b_{ef}^2 \varphi, \end{aligned} \tag{28}$$

where unit contact stiffness k_I is supposed constant and the angles of relative turning of interface surfaces are marked as φ and ϑ. Two flexural contact stiffnesses are then

$$k_{\xi\xi} = \frac{1}{12} k_\zeta \left(h\gamma_h\right)^2, \qquad k_{\eta\eta} = \frac{1}{12} k_\zeta \left(b\gamma_b\right)^2. \tag{29}$$

4. The modelling of bladed disk with damping elements in blade shroud

The motion equations of the fictive undamped system assembled from uncoupled subsystems – the central clamped disk with rigid blade roots and blade rim with damping elements in shroud – in the configuration space

$$\boldsymbol{q} = \left[\left(\boldsymbol{q}_D^{(F)}\right)^T \left(\boldsymbol{q}_D^{(C)}\right)^T \boldsymbol{q}_R^T \right]^T \tag{30}$$

can be formally rewritten as

$$\boldsymbol{M}\ddot{\boldsymbol{q}}(t) + \omega \boldsymbol{G}\dot{\boldsymbol{q}}(t) + \left(\boldsymbol{K}_s + \omega^2 \boldsymbol{K}_\omega - \omega^2 \boldsymbol{K}_d\right) \boldsymbol{q}(t) = \omega^2 \boldsymbol{f}. \tag{31}$$

According to mathematical models (2) and (23), all matrices have the block-diagonal form

$$\begin{gathered} \boldsymbol{X} = \mathrm{diag}\left(\boldsymbol{X}_D,\ \boldsymbol{X}_R\right),\ \boldsymbol{X} = \boldsymbol{M},\ \boldsymbol{G},\ \boldsymbol{K}_d, \\ \boldsymbol{K}_s = \mathrm{diag}(\boldsymbol{K}_{sD},\ \boldsymbol{K}_{sR} + \boldsymbol{K}_C^{(R)}),\ \boldsymbol{K}_\omega = \mathrm{diag}(\boldsymbol{0},\ \boldsymbol{K}_{\omega R}) \end{gathered} \tag{32}$$

and $\boldsymbol{f} = \left[\boldsymbol{f}_D^T,\ \boldsymbol{f}_R^T\right]^T$. The vector of generalized coordinates $\boldsymbol{q}(t)$ of the real bladed disk in consequence of the couplings (6) can be transformed into new vector $\tilde{\boldsymbol{q}}$ in the form

$$\begin{bmatrix} \boldsymbol{q}_D^{(F)} \\ \boldsymbol{q}_D^{(C)} \\ \boldsymbol{q}_R \end{bmatrix} = \begin{bmatrix} \boldsymbol{E} & \boldsymbol{0} \\ \boldsymbol{0} & \boldsymbol{T}_{D,R} \\ \boldsymbol{0} & \boldsymbol{E} \end{bmatrix} \begin{bmatrix} \boldsymbol{q}_D^{(F)} \\ \boldsymbol{q}_R \end{bmatrix} \text{ or shortly } \boldsymbol{q} = \boldsymbol{T}\tilde{\boldsymbol{q}}. \tag{33}$$

The mathematical model of the central clamped bladed disk with damping elements in blade shroud in the configuration space $\tilde{\boldsymbol{q}}$ takes the form

$$\tilde{\boldsymbol{M}}\ddot{\tilde{\boldsymbol{q}}}(t) + \omega\tilde{\boldsymbol{G}}\dot{\tilde{\boldsymbol{q}}}(t) + \left(\tilde{\boldsymbol{K}}_s + \omega^2\tilde{\boldsymbol{K}}_\omega - \omega^2\tilde{\boldsymbol{K}}_d\right)\tilde{\boldsymbol{q}}(t) = \omega^2\tilde{\boldsymbol{f}}, \tag{34}$$

where $\tilde{\boldsymbol{X}} = \boldsymbol{T}^T\boldsymbol{X}\boldsymbol{T}$, $\boldsymbol{X} = \boldsymbol{M}, \boldsymbol{G}, \boldsymbol{K}_s, \boldsymbol{K}_d, \boldsymbol{K}_\omega$ and $\tilde{\boldsymbol{f}} = \boldsymbol{T}^T\boldsymbol{f}$.

5. Modal analysis of bladed disk

The results of blade and shrouded blade modelling was compared with results from commercial software ANSYS. For illustration we present in tab. 3 a number of lowest natural frequencies of the one modeled blade with shroud fixed in the first node on the rigid disk with rigid blade roots. The DOF number of 1D blade model is 36 without reduction (see fig. 5). The first and second natural frequencies are sufficiently accurate, moreover the influence of rotation is practically same also for higher frequencies.

Table 3. Modal analysis of the blade with shroud in different FEM softwares

Frequencies of blade with shroud			
ANSYS	MATLAB	ANSYS	MATLAB
0 rpm		2 000 rpm	
142	141	153	151
282	282	288	286
970,5	1 003	981,5	1 011
1 536	1 533	1 537	1 533
1 907	1 969	1 913	1 974

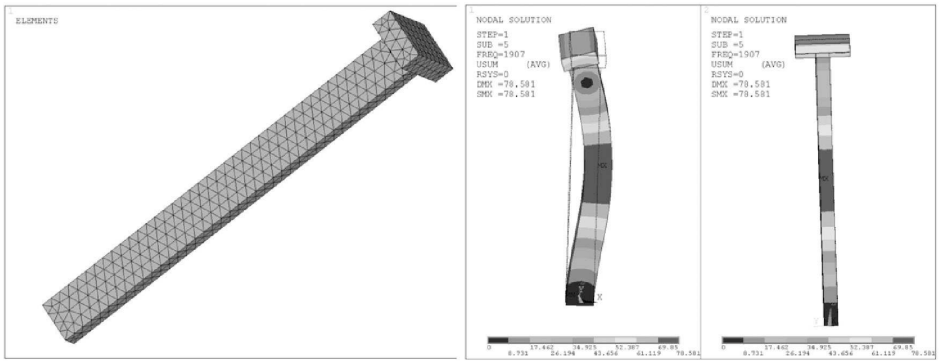

Fig. 5. Model in Ansys (left picture) and model scheme in MATLAB (right picture)

The next step of the testing of the presented method was modal analysis of blade rim, i.e. the blades with shroud connected by contact stiffness matrix $\boldsymbol{K}_R^{(C)}$ of damping elements.The results of modal analysis in the form of the some few lowest natural frequencies of the the blade rim fixed in the first nodes of all blades into rigid disk with rigid blade roots are presented in tab. 4.

Table 4. Modal analysis of the blade rim

Frequencies of blade rim			
Fixed in 1st nodes of blandes		Fixed in 1st nodes of blandes	
0 rpm		2 000 rpm	
[Hz]	number	[Hz]	number
142	60×	151	60×
291	1×	295	1×
618	2×	620	2×
1 003	60×	1 011	60×
1 068	2×	1 069	2×
1 390	2×	1 392	2×

All blades of the blade rim with damping elements are connected with disk rigid foots in the first nodes and the mathematical model (34) of the bladed disk is used for testing. Its modal analysis is performed for undermentioned parameters:

$\delta_a = 20°$ (angle of damping element slope)
$\delta_A = 3.45°$ (angle between radial blade axis x_{i+1} and axis ξ_i)
$\delta_B = 2.55°$ (angle between radial blade axis x_i and axis ξ_i)
$m_T = 0.008\,6$ kg (mass of damping element)
$r_T = 0.465\,5$ m (distance of the centre of gravity of damping element from the rotation axis)
$c = 3$ (contact deformation coefficient)
$p = 0.5$ (contact exponent)
$b = 0.006$ m (radial proportion of damping element)
$h = 0.02$ m (axial proportion of damping element)
$\gamma_b = 0.5$ (coefficient of contact area reduction in radial proportion)
$\gamma_h = 0.5$ (coefficient of contact area reduction in axial direction).

The some few lowest natural frequencies of the central clamped blade disk with damping elements in the blade shroud are presented in tab. 5. The corresponding mode shapes are characterized by the number of nodal diameters ND and nodal circles NC, i.e. the number of lines (resp. circles) with zero amplitude. The graphic demonstration of mode shapes is available but in this paper in gray-scale there are presented for illustration only chosen shapes depicted without shroud and damping elements (see fig. 6–8).

Table 5. Eigenfrequencies of bladed disk – clamped on inner radius

Frequencies of bladed disk Clamped in inner disk radius					
0 rpm			2 000 rpm		
[Hz]	number	shape	[Hz]	number	shape
69,5	2×	1 ND	75,9	2	1 ND
71,7	1×	1 NC	78,3	1	1 NC
84,6	2×	2 ND	91,2	2	2 ND
113,2	2×	3 ND	121,8	2	3 ND
125,5	2×	4 ND	135,0	2	4 ND
130,1	2×	5 ND	140,0	2	5 ND

Fig. 6. Mode shape corresponding to eigenfrequency 69,5 Hz – 1 ND for non-rotating bladed disk

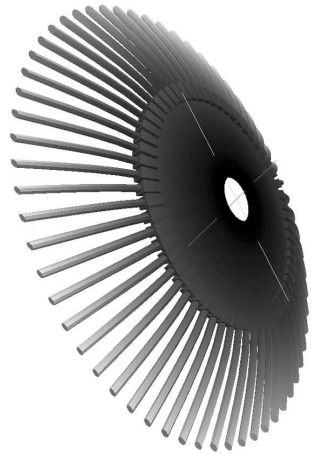

Fig. 7. Mode shape corresponding to eigenfrequency 71,7 Hz – 0 ND for non-rotating bladed disk

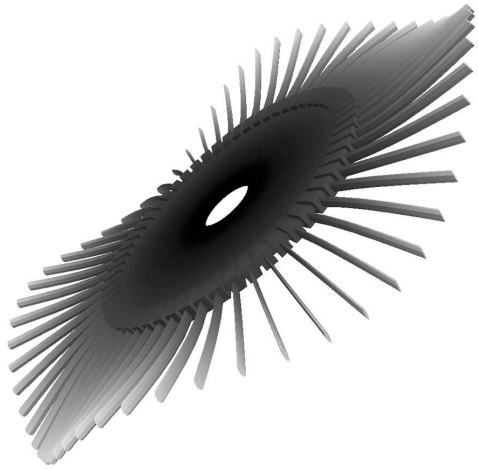

Fig. 8. Mode shape corresponding to eigenfrequency 125,5 Hz – 4 ND for non-rotating bladed disk

6. Conclusion

The presented method and the corresponding developed software enables to create small computational consuming model of the bladed disk for nonlinear task. The disk is modelled as a three dimensional rotating continuum and blades as a one dimensional continuum with rigid shroud connected by damping elements. The displacements of the coupled disk nodes on the rigid blade foots are eliminated by means of displacements in the first blade nodes. The contact stiffnesses of a damping elements supported between blade shroud are respected in sliding interface surfaces. In presented stage of modelling the contact surfaces are considered as smooth. The method allows to introduce continuously distributed centrifugal and gyroscopic effects which influence the bladed disk modal properties. Modal values of particular compo-

nents of the complete model were compared with modal values calculated using commercial software. The modal accurance is good. The model is prepared for including damping effects. In future, the forced vibration and its graphical representation will be done. The model does not use the cyclic symmetry and is prepared for system with different blades (with and without shroud).

The new approach to bladed disk vibration modelling was tested for undamped modeled bladed disk with sixty blades and damping elements. From a modal analysis follows that the developed software in MATLAB code based on presented methodology is acceptable for a modelling of damping effects.

Acknowledgements

This work was supported by GA CR in the project No. 101/09/1166 “Research of the dynamic behaviour and optimization of complex rotating system with non-linear couplings and high damping materials” and the research project MSM 49 777 513 03 supported by the Ministry of Education, Youth and Sports of the Czech Republic.

References

[1] Šašek, J., Zeman, V., Hajžman, M., Modal properties of rotating disks. Proceedings of the 22nd Computational Mechanicss 2006, University of West Bohemia, Vol. 2, pp. 593–600.

[2] Rao, S. S., The finite element method of engineering. Oxford: Pergamon Press, 1989.

[3] Kellner, J., Zeman, V., Infuences of dynamic stiffnes, centrifugal forces and blade’s elastic seating on blade modal properties, Proceedings of the 8th Applied Mechanics 2006, University of West Bohemia in Pilsen, pp. 47–48.

[4] Zeman, V., Šašek, J., Byrtus, M., Modelling of rotating disk vibration with fixed blades, Modelling and optimization of physical systems 8 (2009), Silesian University of Technology, Gliwice, pp. 125–130.

[5] Kellner, J., Vibration of turbine blades and bladed disks (in Czech), Doctoral thesis, University of West Bohemia in Pilsen, 2009.

[6] Riwin, E. I., Stiffness and damping in mechanical design, Wayne state university Detroit, Michigan, New York 1999.